



# BIOMECHANICAL PROPERTIES OF FIXED-ANGLE VOLAR DISTAL RADIUS PLATES UNDER DYNAMIC LOADING

Orthopaedic Research Laboratories  
Lutheran Hospital  
a Cleveland Clinic hospital  
Cleveland, Ohio

Paul D. Postak, B.Sc.  
A. Seth Greenwald, D.Phil.(Oxon)

Cleveland Clinic  
Department of Orthopaedic Surgery  
Cleveland, Ohio

Paul Nassab, M.D.  
Jeffrey Lawton, M.D.  
Peter Evans, M.D.

Cleveland Orthopaedic and  
Spine Hospital at Lutheran  
Cleveland Clinic  
Cleveland, Ohio

William H. Seitz, Jr., M.D.  
Craig Burgess, D.O.

## INTRODUCTION

Distal radius fractures are commonly encountered in general orthopaedic and hand subspecialty practices (Figure 1). Most surgeons are comfortable with both operative and nonoperative management of these fractures. Treatment options have evolved with fracture pattern governing the specific treatment modality. Casting with or without reduction, percutaneous pinning, external fixation, and open reduction with internal fixation employing dorsal, volar and fragment specific plates are all common methods used to treat these injuries.

A paradigm shift has occurred in the treatment of dorsally displaced distal radius fractures. Previous volar plating techniques demonstrated a high failure rate when compared to dorsal buttress plating which prevented fracture settling and recurrent displacement. Orbay<sup>7</sup> and others have developed volar plating constructs, which provide subchondral support to the distal radius, transferring radiocarpal forces experienced in the postoperative period to the plate and volar cortex. Previous studies have examined biomechanical differences between dorsal and volar plating while further investigations between specific volar plate constructs under static and dynamic loading conditions have been reported.<sup>1-5,8,9,11,14,15,17</sup>

This study compares the biomechanical properties of eight different fixed-angle volar distal radius plate designs under dynamic loading to determine their ability to withstand the forces which occur during fracture healing and early postoperative rehabilitation. The **Acumed**<sup>®</sup> Acu-Loc<sup>™</sup> (Acumed, Hillsboro, OR), **Hand Innovations**<sup>®</sup> DVR<sup>™</sup> (Hand Innovations, Miami, FL), **SBi**<sup>®</sup> SCST<sup>™</sup> Volar Distal Radial Plate (Small Bone Innovations, Morrisville, PA), **Synthes**<sup>®</sup> Volar Distal Radius Plate (Synthes, Paoli, PA), **Synthes**<sup>®</sup> EA Extra-Articular Volar Distal Radius Plate (Synthes, Paoli, PA), **Stryker**<sup>®</sup> Matrix-SmartLock<sup>™</sup> (Stryker Leibinger, Kalamazoo, MI), **Wright** Medical Technology Locon VLS<sup>™</sup> (Wright Medical Technology, Arlington, TN), and **Zimmer** Periarticular Distal Radius Locking Plate (Zimmer, Warsaw, IN) were all evaluated.



Figure 1: PA, lateral and oblique radiographs of a distal radius fracture in a 62-year-old male.

# MATERIALS AND METHODS

## *Plate Application*

For each of the eight plate designs, seven third-generation synthetic composite bone radii (Pacific Research Laboratories, Inc., Vashon, WA) were fitted with fixed-angle plates according to the manufacturers' recommended techniques (Figure 2). Hardware representatives were present from each company for the application of their respective plate system for six plate designs. For the remaining two designs, the **Acumed**<sup>®</sup> Acu-Loc<sup>™</sup> and the **SBi**<sup>®</sup> SCST<sup>™</sup> Volar Distal Radial Plates, the synthetic composite bone specimens were mailed to representatives from each company who placed their plates on the synthetic composite bone radii. Acumed preferred to place their plates because they required bending to meet the specific volar anatomy of the radius. No attempt was made to bend any other plate system to conform to the distal radial anatomy.

Five designs tested had distal locking screws which locked into pre-threaded distal screw holes in the plate (**Acumed**<sup>®</sup> Acu-Loc<sup>™</sup>, **Synthes**<sup>®</sup> Volar Distal Radius Plate, **Synthes**<sup>®</sup> EA Extra-Articular Volar Distal Radius Plate, **Wright** Medical Technology Locon VLS<sup>™</sup>, and **Zimmer** Periarticular Distal Radius Locking Plate). The **Stryker**<sup>®</sup> Matrix-SmartLock<sup>™</sup> system differed in that the locking screws tapped their threads into the plate as they were placed. The **Hand Innovations**<sup>®</sup> DVR<sup>™</sup> system differed in that pegs were used rather than locking screws to fix the distal portion and the **SBi**<sup>®</sup> SCST<sup>™</sup> Volar Distal Radial Plate has fixed-angle tines, not screws. The placement of all plates and screws is shown below and was guided by the desire to maximize the support of subchondral bone.



*Acumed*



*Hand Innovations*



*SBi*



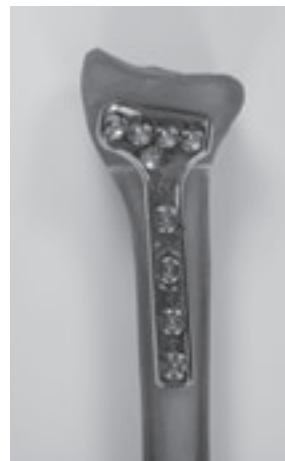
*Synthes*



*Synthes EA*



*Stryker*



*Wright*



*Zimmer*

*Figure 2: Contemporary fixed-angle volar distal radius plate designs evaluated in this study.*

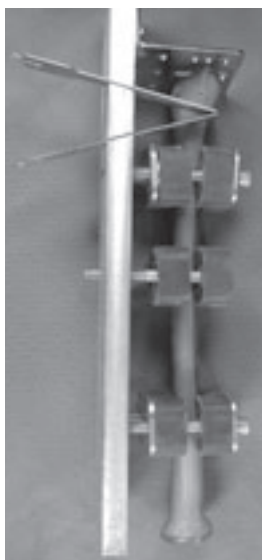


*Figure 3: Custom osteotomy fixture: Blades in place converge on the volar cortex of the synthetic composite bone.*

### *Osteotomy and Specimen Preparation*

A one centimeter dorsal wedge osteotomy was made in the plate-synthetic composite bone construct with a Stryker 4000 saw (Stryker Leibinger, Kalamazoo, MI) (Figure 3). A custom fixture was fabricated to standardize the osteotomy. The volar cortex was scored but not violated. The osteotomy of the volar cortex was completed with a fine file by hand. Care was taken not to damage the plate. Three millimeter diameter stainless steel beads were fixed to the proximal and distal radial and ulnar margins of the osteotomy to allow measurement of settlement or collapse of the distal radius between testing phases. A fine permanent marker was used to orient the distal locking screw to the plate. This was done to help establish if the screws loosened after cyclic testing.

### *Biomechanical Testing*

Each construct was tested on a Materials Testing System (MTS, Eden Prairie, MN) (Figure 4). The proximal ends were potted in a reusable acrylic mold of the synthetic composite bone radius. An axial load was applied through an acrylic model of the scaphoid and lunate bones, molded from a cadaveric wrist.



*Figure 4: Plate-synthetic composite bone construct on MTS. Note osteotomy and beads for measurements.*

Three separate testing phases were performed on each specimen to simulate both the number of cycles and magnitudes of force that the plate-bone construct would experience over a 6-week period of fracture healing.<sup>11</sup> The specimen was preloaded to 10 Newtons (N) during each phase and then loaded to 100N, 200N and 300N in Phases 1, 2 and 3, respectively, at a rate of 2N/s. Each construct was then dynamically loaded for 2000 cycles at a frequency of 2Hz in each phase, for a total of 6000 cycles. Each specimen was then loaded to failure at 2N/s.

### *Measurements*

The following measurements and observations were made:

- Load-deformation curves were determined for each of the three phases in all specimens.
- Yield strength calculated from the load to failure curve.
- The distances between the edges of the osteotomy sites were measured between each phase to establish if settling had occurred.
- Each distal screw/hole marker was inspected to see if screw loosening had occurred. A screwdriver was not placed into the screws to check for loosening.

## **RESULTS**

Figures 5 and 6 graphically illustrate the stiffness for each plate design. All constructs were stiffer at higher loads. All plates tested had an initial stiffness on the order of 150N/mm at 100N. This increased to over 300N/mm at 300N with the **Hand Innovations**<sup>®</sup> DVR<sup>™</sup>, **Stryker**<sup>®</sup> Matrix-SmartLock<sup>™</sup>, and **Wright** Medical Technology Locon VLS<sup>™</sup> plates. No plates failed during any aspect of the testing.

Yield strengths are illustrated in Figure 7. The **Zimmer** Periarticular Distal Radius Locking and **Hand Innovations**<sup>®</sup> DVR<sup>™</sup> plates had the highest yield strengths while the **Wright** Medical Technology Locon VLS<sup>™</sup>, **SBi**<sup>®</sup> SCS<sup>™</sup> Volar Distal Radial, **Stryker**<sup>®</sup> Matrix-SmartLock<sup>™</sup>, and **Synthes**<sup>®</sup> EA Extra-Articular Volar Distal Radius plates had the lowest yield strengths. Plate design appeared more important than material as both stainless steel and titanium plates were among the strongest and weakest plates.

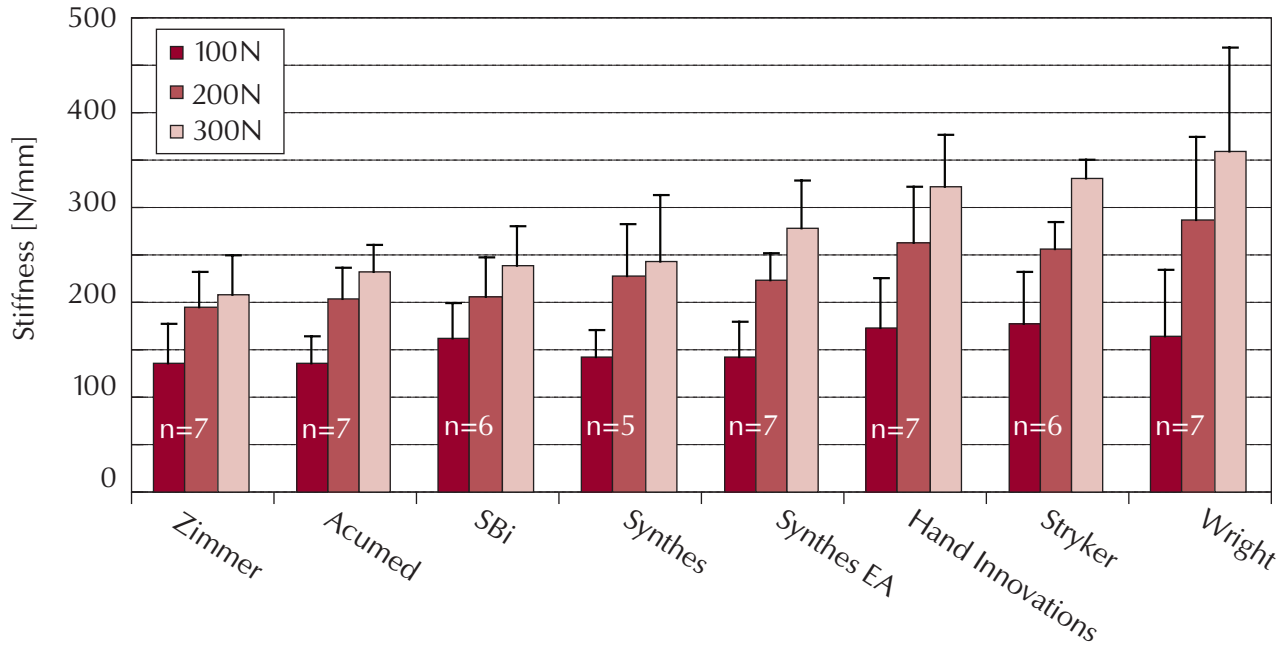


Figure 5: Graph of average volar plate stiffness with standard deviations at 100N, 200N, and 300N load levels that demonstrates an increase in stiffness with increasing load. Differences in average stiffness between plate designs was investigated with the Tukey-Kramer multiple comparison ANOVA test at each load level. Significant differences were found at the 100N level with the Wright plate being stiffer than Zimmer plate ( $p < 0.05$ ). No differences between the plate designs were found at the 200N load level. Significant differences were found at the 300N level with the Wright plate being stiffer than four other plate designs: Zimmer ( $p < 0.001$ ), Acumed ( $p < 0.01$ ), SBi ( $p < 0.05$ ), and Synthes ( $p < 0.05$ ). At 300N the Zimmer plate was also significantly more compliant than two other plate designs: Stryker ( $p < 0.05$ ) and Hand Innovations ( $p < 0.05$ ).

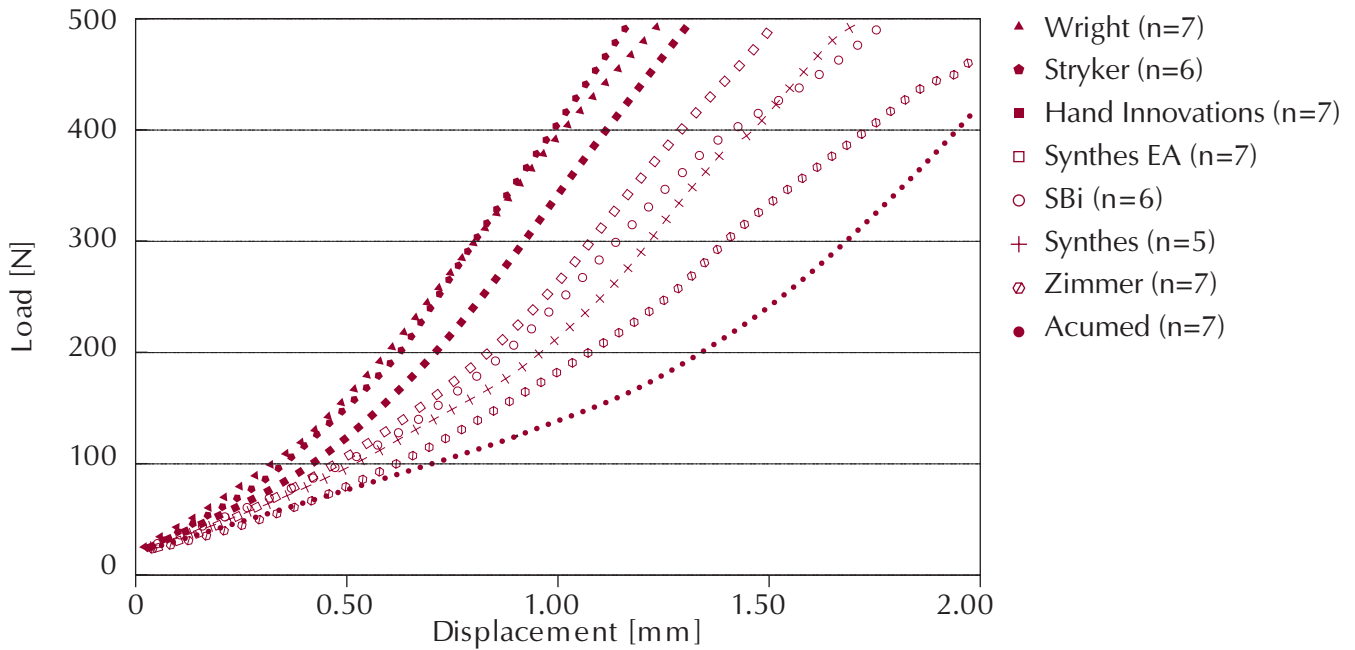


Figure 6: Graph of the average displacement response of all plate designs after 6000 cycles demonstrating stiffness differences in the range of expected postoperative loading.

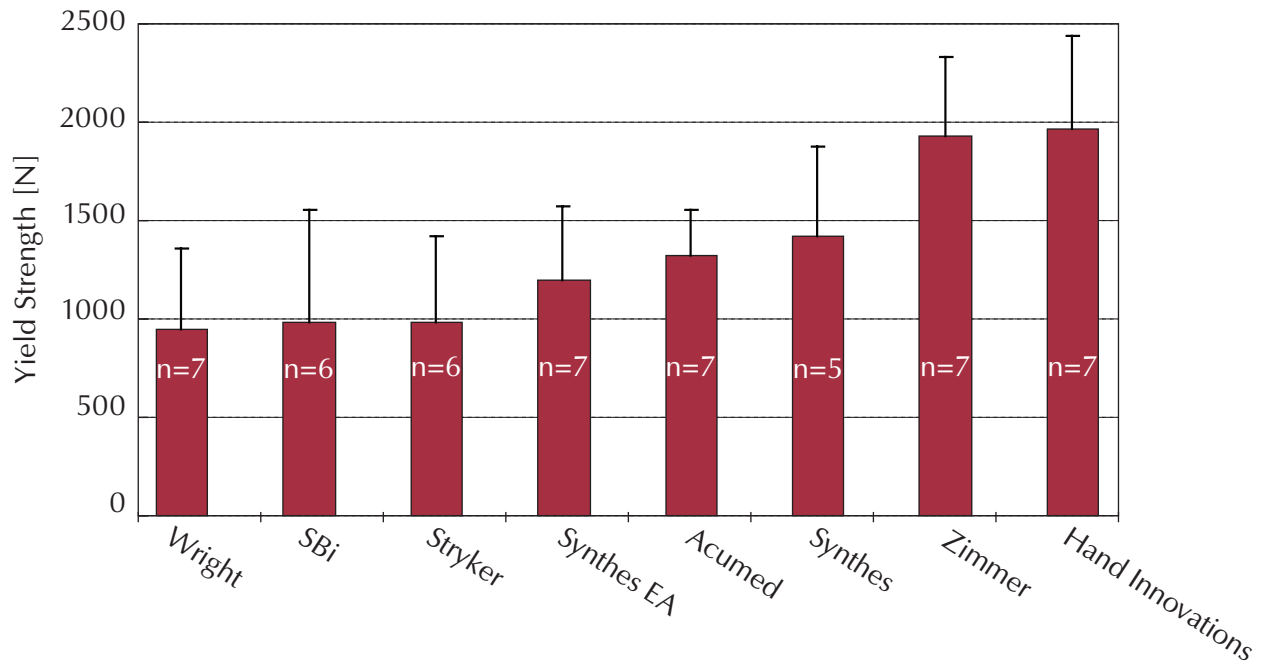


Figure 7: Graph of average volar plate yield strength with standard deviations. Differences in average yield strength between plate designs was investigated with the Tukey-Kramer multiple comparison ANOVA test at each load level. Significant differences were found with the Zimmer and Hand Innovations designs yielding at higher loads when compared to four other designs: Wright ( $p < 0.01$ ), SBi ( $p < 0.01$ ), Stryker ( $p < 0.01$ ), and Synthes EA ( $p < 0.05$ ).

The fracture margin distances did not decrease for any of the plate designs evaluated. In other words, no deformation of the plate, screws or synthetic composite bone after any of the cyclic testing was observed in any of the constructs. Similarly, loosening of any locked screw in the distal fragment of the tested constructs was not identified.

## DISCUSSION

This study provides quantitative, comparative and descriptive data for eight different fixed-angle volar plate systems used to treat distal radius fractures. Similar studies have been performed in the past although many have compared dorsal versus volar plating and the majority has focused on results with non-cyclic testing.<sup>1-5,8,9,11,15,17</sup> We chose to perform dynamic testing to simulate the *in vivo* postoperative forces to which these plates would be exposed. Dynamic testing simulates early postoperative rehabilitation protocols aimed at decreasing edema and increasing postoperative range of motion.<sup>13</sup>

Putnam et al<sup>11</sup> have shown that 26N of force is transmitted across the distal radius for every 10N of grip strength in a cadaveric model. The 50/50 distribution of forces across the radius and ulna in this study did not reflect the approximately 80/20 ratio that has been reported by others.<sup>1,10,16</sup> The distal radius would see 41.9N of force for every 10N of grip strength if one assumes that 80 percent, not 50 percent, of the load is transmitted across the distal radius. Cyclic loading of 100N, 200N, and 300N across the distal radius in our study would therefore correspond to grip strengths of 24N, 48N, and 72N, respectively.

Mathiowetz et al<sup>6</sup> established average maximal grip strengths in a diverse study population. The average grip strength for males was 463N which would distribute 1940N across the distal radius. Our results show that these plates fail in a range from 1000N to 2000N after cyclic testing. Rozental and Blazar<sup>12</sup> have reported an average maximal grip strength of 94% of the unaffected side seventeen months after volar plate fixation for distal radius fractures. Certainly maximal grip can risk fracture fixation and result in plate-synthetic composite bone failure. Alternatively, however, common sense and clinical experience dictate that patients are not capable

of maximal grip for many weeks postoperatively. The current data show that these plates can withstand forces encountered with normal wrist flexion and extension and repetitive sub-maximal finger flexion and extension. One would expect that the plate-bone construct would be offloaded somewhat by the healing fracture by the time patients are capable of generating greater forces.

It is clear that the plate-synthetic composite bone construct was exposed to forces transmitted across the wrist and did not fail under any of the sub-maximal testing phases.

## TAKE HOME MESSAGE

- There are significant differences in the yield strengths between several of the plate designs evaluated. However, all plates tested failed at loads above what is considered physiologic during the postoperative healing phase through fracture union.
- No distal locking screw loosening occurred prior to bone-plate construct failure.
- Fracture pattern and screw configuration may be more important than biomechanical differences between plates and should guide plate selection for fracture fixation.
- All factors being equal, ease of use, physician comfort with technique, hardware availability, and cost may be the most important factors when choosing a volar plate system for dorsally displaced, extra-articular distal radius fractures.

## REFERENCES

1. Ekenstam, F.W., Palmer, A.K., and Glisson, R.R., The load on the radius and ulna in different positions of the wrist and forearm. A cadaver study. *Acta Orthop Scand*, 1984. **55**(3): p. 363-5.
2. Gesensway, D., et al., Design and biomechanics of a plate for the distal radius. *J Hand Surg [Am]*, 1995. **20**(6): p. 1021-7.
3. Koh, S., et al., Volar fixation for dorsally angulated extra-articular fractures of the distal radius: a biomechanical study. *J Hand Surg [Am]*, 2006. **31**(5): p. 771-9.
4. Leung, F., et al., Palmar plate fixation of AO type C2 fracture of distal radius using a locking compression plate--a biomechanical study in a cadaveric model. *J Hand Surg [Br]*, 2003. **28**(3): p. 263-6.
5. Liporace, F.A., et al., A biomechanical comparison of a dorsal 3.5-mm T-plate and a volar fixed-angle plate in a model of dorsally unstable distal radius fractures. *J Orthop Trauma*, 2005. **19**(3): p. 187-91.
6. Mathiowetz, V., et al., Grip and pinch strength: normative data for adults. *Arch Phys Med Rehabil*, 1985. **66**(2): p. 69-74.
7. Orbay, J.L., The treatment of unstable distal radius fractures with volar fixation. *Hand Surg*, 2000. **5**(2): p. 103-12.
8. Osada, D., et al., Biomechanics in uniaxial compression of three distal radius volar plates. *J Hand Surg [Am]*, 2004. **29**(3): p. 446-51.
9. Osada, D., et al., Comparison of different distal radius dorsal and volar fracture fixation plates: a biomechanical study. *J Hand Surg [Am]*, 2003. **28**(1): p. 94-104.
10. Palmer, A.K. and Werner, F.W., Biomechanics of the distal radioulnar joint. *Clin Orthop Relat Res*, 1984(187): p. 26-35.
11. Putnam, M.D., et al., Distal radial metaphyseal forces in an extrinsic grip model: implications for postfracture rehabilitation. *J Hand Surg [Am]*, 2000. **25**(3): p. 469-75.
12. Rozenal, T.D. and Blazar, P.E., Functional outcome and complications after volar plating for dorsally displaced, unstable fractures of the distal radius. *J Hand Surg [Am]*, 2006. **31**(3): p. 359-65.
13. Slutsky, D.J. and Herman, M., Rehabilitation of distal radius fractures: a biomechanical guide. *Hand Clin*, 2005. **21**(3): p. 455-68.
14. Taylor, K.F., Parks, B.G., and Segalman, K.A., Biomechanical stability of a fixed-angle volar plate versus fragment-specific fixation system: cyclic testing in a C2-type distal radius cadaver fracture model. *J Hand Surg [Am]*, 2006. **31**(3): p. 373-81.
15. Trease, C., McCliff, T., and Toby, E.B., Locking versus nonlocking T-plates for dorsal and volar fixation of dorsally comminuted distal radius fractures: a biomechanical study. *J Hand Surg [Am]*, 2005. **30**(4): p. 756-63.
16. Trumble, T., et al., Forearm force transmission after surgical treatment of distal radioulnar joint disorders. *J Hand Surg [Am]*, 1987. **12**(2): p. 196-202.
17. Yetkinler, D.N., et al., Biomechanical evaluation of fixation of intra-articular fractures of the distal part of the radius in cadavera: Kirschner wires compared with calcium-phosphate bone cement. *J Bone Joint Surg Am*, 1999. **81**(3): p. 391-9.